Invisibility and supervisibility: Radiation dynamics in a discrete electromagnetic cloak

Adel Rahmani,[1] M. J. Steel,[2] and Patrick C. Chaumet[3]

[1]*School of Mathematical Sciences, University of Technology, Sydney, Broadway NSW 2007, Australia*
[2]*MQ Photonics and Centre for Ultrahigh bandwidth Devices for Optical Systems (CUDOS), Department of Physics and Astronomy, Macquarie University, NSW 2109 Australia*
[3]*Institut Fresnel, CNRS, Aix-Marseille Université, Campus de St-Jérôme 13013 Marseille, France*

We study the radiation dynamics of an electric dipole source placed near or inside a discrete invisibility cloak. We show that the main features of radiation dynamics can be understood in terms of the interaction of the source with a nonideal cloak in which local-field effects associated with the discrete geometry play a crucial role. As a result, radiation dynamics in a discrete cloak can differ drastically from what a source would experience in an ideal, continuous cloak. This can lead, for instance, to an enhancement of the emission by the cloak, thus making the source more visible to an outside observer than it would be without the cloak. The two main physical mechanisms for enhanced, or inhibited, radiation dynamics are the coupling of the source to leaky modes inside the cloak, and the coupling of the source with the lattice of the discrete cloak, via the local field. We also explore the robustness of the effect to material dispersion and losses.

PACS number(s): 41.20.Jb, 42.25.Fx, 42.25.Gy, 78.67.Pt

I. INTRODUCTION

The influence of the environment on the emission rate of an electromagnetic source is a well-known and widely exploited concept in photonics and quantum optics.[1,2] The radiation dynamics of a source can be enhanced, or inhibited, by a suitable design of the environment of the source. In this article, we are interested in the radiation dynamics of a source placed inside a spherical or cylindrical cloaking device of the transformation optics class.[3–5] Specifically, we seek to find out the qualitative aspects of radiation dynamics for a source placed in a *nonideal* cloaking device, in particular, nonideality associated with the discrete construction of the cloak. This is an important point because whereas the material properties (or equivalently, the geometry of space) associated with cloaking are derived for a continuum, at this time, transformation optics cloaking devices operating in the optical domain can only be fabricated using a discrete geometry.[5] This discrete geometry will compromise the cloaking device's ability to perfectly hide an object (or itself) from an electromagnetic probe. In other words, whereas an ideal cloak separates space into two regions that do not couple electromagnetically, due to its discrete (i.e., composite) structure any real cloaking device would exhibit some amount of electromagnetic "leakage" between its interior region and the outside world. As we will see, this discrete structure is responsible for some interesting radiation dynamics.

Of course, by now there has been a wide variety of strategies proposed and demonstrated for implementing electromagnetic cloaking. Some authors have suggested ingenious cloaking strategies that manage to avoid (lossy) metallic components or strongly subwavelength features altogether; these include the mapping of anisotropic responses to tapered conventional waveguides,[6] and the use of macroscopic birefringent materials.[7–9] By and large, however, one can choose from cloaking by anomalous plasmonic resonance,[10–13] scattering cancellation by shells of near-zero or negative permittivity materials[14–16] (both typically involving lossy metals), or the transformation optics approach,[3–5,17–19] which generally requires metamaterials to provide the required strong anisotropy and singular responses. Within the latter class, the concept of carpet cloaking[20] has substantially eased requirements on anisotropy and singular responses allowing convincing microwave[21,22] and optical demonstrations in two[23–25] and three[26,27] dimensions. Nonetheless, despite the less extreme material properties, which can be attained using dielectrics, the required smooth variation in refractive index is still typically accomplished through periodic or quasiperiodic structures (arrays of discrete holes or pillars,[23,24] or modulated photonic crystals[26,28]). A unique aspect of the vanilla transformation optics as opposed to the plasmonic techniques or carpet cloaking is that in the former, the interior and exterior regions of the cloak are, at least formally, completely decoupled. In contrast, some plasmonic shell style cloaks, with thin layers of low or negative permittivity, allow almost perfect cancellation of scattering by a cloaked sensor, and yet external radiation is clearly detectable by the sensor.[16,29,30] In such cases, however, the shell must be designed for the cloaked object whereas the requirements for decoupled spaces in the transformation optics picture are agnostic about the electromagnetic properties of the cloaked object. Here, we restrict consideration to transformation optics cloaks where in the ideal scenario the external and internal regions are completely separate.

If the design of the shell departs from the ideal prescription for the permittivity and permeability, the cloaking mechanism is only approximate. Scattering of *external* light by approximate cloaks has been the subject of several recent studies.[31–35] In the context of transformation optics, approximate cloaking usually involves a modification of the constitutive material properties of the cloak (e.g., altered boundary condition or simplified material parameters). The main consequence of approximate cloaking is that the presence of the imperfect cloak can be detected through its scattering signature. In this context, an original and interesting study has considered the detection of *arrays* of cloak structures by their dispersive response rather than far-field scattering.[36,37] An array of ideal cloaks would induce a vacuum Bloch wave band structure, but

imperfect cloaks associated with a layered physical system, show a departure from the vacuum response.[37] In particular, the imperfect cloaks support quasitrapped states, which have a clear signature in the form of a flat Bloch mode. These modes are almost dispersionless due to weak coupling between the imperfect cloaks. The array also supports Mie-like resonances at each cloak site. As we shall see, for a single cloak, the presence of these leaky modes leads to some interesting radiation dynamics for a source inside the cloak.

While most attention in the transformation optics cloaking literature is on scattering of external fields, the nominal separation of interior and exterior makes the behavior of a dipole source inside the cloak especially interesting. Zhang *et al.*,[38] for example, showed that a source in an ideal continuum cloak leads to unusual surface voltages that "implement" the hiding of the source. As already mentioned, in practice, the anisotropy required by cloaking structures is achieved through metamaterials: periodic multicomponent structures, which can have quite complex geometries.[39] At least in the optical regime, for the foreseeable future, the ratio of the wavelength λ to the periodicity scale d will be quite modest, say λ/d in the range (20,50). Thus while models of cloaks generally assume a continuum description of the medium (as do the techniques of transformation optics from which they are derived[40]), it is important to consider the impact of the discrete nature of the metamaterials on the behavior of the cloak. Accordingly, in this paper, our focus is explicitly on how the discreteness associated with a metamaterial implementation of the cloak impacts the radiation dynamics of a source inside the cloak. Note that in contrast to other approaches, we start with the full, anisotropic electric, and magnetic responses of an ideal cloak and we incorporate into the model a discrete geometry. Aside from introducing changes in the overall electromagnetic response of the cloak (compared to the ideal, continuous model), the discrete geometry of the metamaterials entails that the radiation properties of a source placed within the metamaterial lattice itself depend on its precise position within the lattice. This effect, which is distinct from the radiation dynamics associated with the overall shape of the cloak, can only be grasped with a discrete model of a cloak.

For any particular implementation, one could numerically model the detailed structure of the metamaterial making up the cloak and determine the effects of discreteness essentially by brute force. Such a task would obviously be time consuming and would be specific to the particular system modelled. Here, we take a more general approach. Instead of dealing with the complexity of any given metamaterial design, we use the discrete dipole approximation (DDA)[41,42] to obtain a simple, yet effective discrete model of a cloak. This approach, which has recently been used to study the optomechanics of a discrete cloak,[43,44] allows us to compute the emission rate of a source self-consistently in the weak-coupling regime, even in the presence of losses.[45–48] It is also ideally suited for considering the local-field effects that arise when the source is in the lattice of the cloak medium. For a source in the presence of a discrete cloak, we will show that the cloak can, as expected, inhibit the emission rate of the source (i.e., reduce the power radiated by the source) but surprisingly, also enhance it.

In Sec. II, we present a discrete dipole model of a spherical, transformation optics cloak. The model is used in Sec. III

to calculate the emission rate of a source in the presence of a discrete cloak. Section IV explains the features of the radiation dynamics of the source in term of coupling to leaky resonances inside the cloak. We consider the effect of material dispersion and losses in Sec. V. Our conclusions are presented in Sec. VI.

II. GENERIC DESCRIPTION OF A COMPOSITE INVISIBILITY CLOAK

In this paper, as an example system, we consider the ideal spherical invisibility cloak introduced by Pendry *et al.*[4] Following the notation of Ref. 49, the cloak is centered on the origin with inner radius a and outer radius b [see inset in Fig. 2(a)]. The electromagnetic response of the cloak is defined by the permittivity and permeability tensors:[49]

$$\bar{\bar{\epsilon}}(\mathbf{r}) = \bar{\bar{\mu}}(\mathbf{r}) = \frac{b}{b-a}\left(\bar{\bar{I}} - \frac{2ar - a^2}{r^4}\mathbf{r}\otimes\mathbf{r}\right), \quad (1)$$

where $\bar{\bar{I}}$ is the identity tensor, $\mathbf{r} = (x,y,z) = r\hat{\mathbf{r}}$ is the position vector and $\otimes$ represents the dyadic outer product. In the DDA, the spherical cloak is discretized over a cubic lattice with spacing d and represented as a collection of polarizable elements. Let k be the wavenumber, each element has electric and magnetic polarizability tensors:[48]

$$\bar{\alpha}_i^{\mathrm{e}} = \left[\bar{\bar{I}} - \tfrac{2}{3}ik^3\bar{\bar{A}}_i\right]^{-1}\bar{\bar{A}}_i, \quad \bar{\alpha}_i^{\mathrm{m}} = \left[\bar{\bar{I}} - \tfrac{2}{3}ik^3\bar{\bar{B}}_i\right]^{-1}\bar{\bar{B}}_i, \quad (2)$$

which are related to the prescribed continuous response functions $\bar{\bar{\epsilon}}$ and $\bar{\bar{\mu}}$ by

$$\bar{\bar{A}}_i = \frac{3d^3}{4\pi}[\bar{\bar{\epsilon}}(\mathbf{r}_i) - \bar{\bar{I}}][\bar{\bar{\epsilon}}(\mathbf{r}_i) + 2\bar{\bar{I}}]^{-1},$$
$$\bar{\bar{B}}_i = \frac{3d^3}{4\pi}[\bar{\bar{\mu}}(\mathbf{r}_i) - \bar{\bar{I}}][\bar{\bar{\mu}}(\mathbf{r}_i) + 2\bar{\bar{I}}]^{-1}. \quad (3)$$

Note that we can account for material dispersion and absorption in the polarizabilities through the response functions, as we shall illustrate in Sec. V. Once the electromagnetic response of each element is known, we can compute the emission rate following the method of Refs. 45,46,48,50. In this way, we aim to capture generic features of a discrete cloak that are not specific to any particular metamaterial implementation. The precise magnitude of effects we observe would of course vary from instance to instance. We highlight that this is a rather unusual application of the DDA. Traditionally the DDA, like most numerical electromagnetic solvers, is used to model nominally continuous structures. Accordingly, one would typically reduce the size of the discretization spacing until some suitable convergence criterion has been achieved. Here, we intentionally use a moderate lattice spacing to highlight qualitatively the influence of the discrete units that make up the metamaterial forming the cloak. In that sense, one can regard each DDA scatterer as corresponding to one nominal metamaterial unit (say a split ring resonator or fishnet unit cell), as illustrated in Fig. 1. At the expense of giving up a precise model of any particular instance of a metamaterial cloak, our approach has a number of advantages: it is highly efficient; we can treat scattering by metallic resonators simply as complex polarizabilities; we can easily account for scattering by source dipoles *within the cloaking material itself* and so
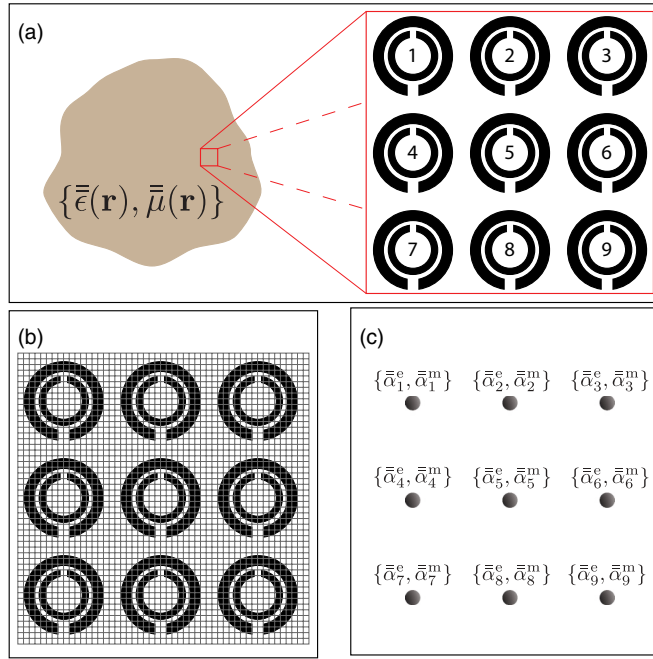
FIG. 1. (Color online) Schematic diagram of discretization in DDA picture. (a) The nominal physical system: a continuum magnetodielectric material implemented by subwavelength resonators. (b) Conventional fine-grained discretization with position dependent responses. (c) High-level discretization with a single pair of polarizability tensors for each resonator.
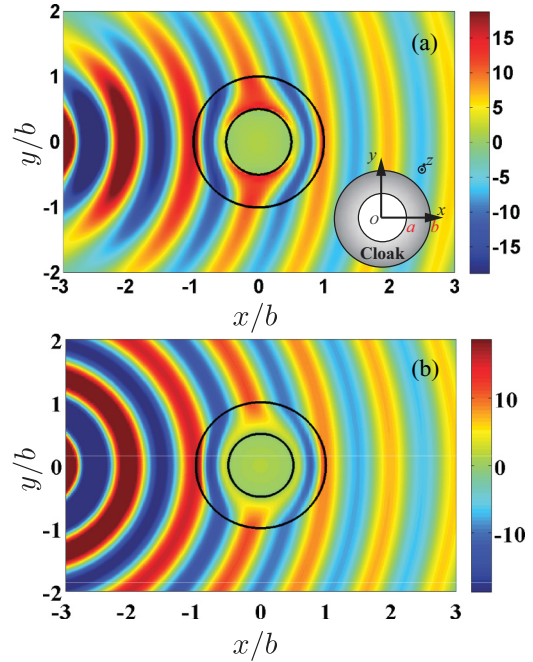

FIG. 2. (Color online) Map of the y (top) and z (bottom) components of the electric field in the $z = 0$ plane (arb. units) for a cloak with $b = 2a$. The wavelength is $\lambda = b$. The source is an electric dipole oriented along y (b) or z (c) and located (outside the domain of the plot) at $(-3.5b, 0, 0)$. The inset shows a cross section of the cloak through the $z = 0$ plane. (The strength of the electric field is arbitrary, being proportional to the strength of the dipole source.)

discuss local-field effects, which do not arise in the continuum treatment.

To illustrate the basic cloaking effect of externally incidence light with a discrete cloak using the DDA, Figs. 2(a) and 2(b) show maps of the electric field in the plane $z = 0$ where the source (not shown) is an electric dipole oriented along y (a) or z (b) and located at $(-3.5b, 0, 0)$. The discretization lattice has spacing $d = \lambda/50$. The effect of the cloak on the wave front of the radiation field of the dipole is clearly visible. Because our cloak is discrete and therefore leaky, the field inside the cloak is not zero although it is reduced by about an order of magnitude compared to what it would be without the cloak. A study of the scattering properties of this type of structure using the DDA can be found in Ref. 51.

III. EMISSION RATE FOR A COMPOSITE INVISIBILITY CLOAK

Now consider an electric dipole source located at $\mathbf{r}_0$ in space, radiating at a wavelength $\lambda = 2\pi/k$. Assuming that the power emitted by the source in free space is Γ_∞, in the presence of the cloak the power radiated by the source, Γ_{cloak}, is, in general, different from Γ_∞. The relative change in radiated power can be expressed as

$$\frac{\Gamma_{\text{cloak}}}{\Gamma_\infty} = 1 + \frac{3}{2k^3}\mathbf{p} \cdot \text{Im}[\bar{\bar{\mathcal{G}}}_{\text{cloak}}(\mathbf{r}_0, \mathbf{r}_0; \omega)] \cdot \mathbf{p}, \qquad (4)$$

where $\bar{\bar{\mathcal{G}}}_{\text{cloak}}$ is the field-susceptibility tensor (FST)[48,52,53] associated with the cloak. Note that the same expression would describe, in the weak coupling regime, the spontaneous emission rate of a quantum source undergoing an electric dipole transition, the imaginary part of the field-susceptibility tensor being proportional to the local density of states at the location of the source.[54] Obviously, a magnetic dipole can be treated in a similar fashion. Hence, the emission rate of a source in an arbitrary environment can be computed provided one knows the corresponding FST. Happily, the FST of a complex structure can be computed using the DDA formalism. Note that one could also compute the field scattered back to the source by the environment and find the resulting work done by the field on the source, which is another interpretation of Eq. (4).

For an ideal cloak, we would expect that the emission rate (power radiated to the far-field) of a classical source would be the same as in free space for a source outside the cloak (or in the cloak shell) and zero for a source inside the cloak (at a distance $r < a$ from the origin). In other words, we expect the cloaking device to act like a perfect cavity.[55] However, here the discrete structure of the cloak results in a coupling (i.e., leakage) between the outer and inner regions. We choose parameters $b = 2\lambda$, $a = \lambda$. As discussed previously, we only need a modest level of discretization to observe the generic behavior of a discrete cloak. We use a lattice spacing $d = b/50$ to have a strong enough cloaking effect to see clearly its consequence on the source. This corresponds to having at most 25 discrete elements in any radial direction across the shell of the cloak. We plot in Fig. 3 the emission rate as a function of the distance of the source from the center of the cloak for two orientations of the dipole moment of the source.
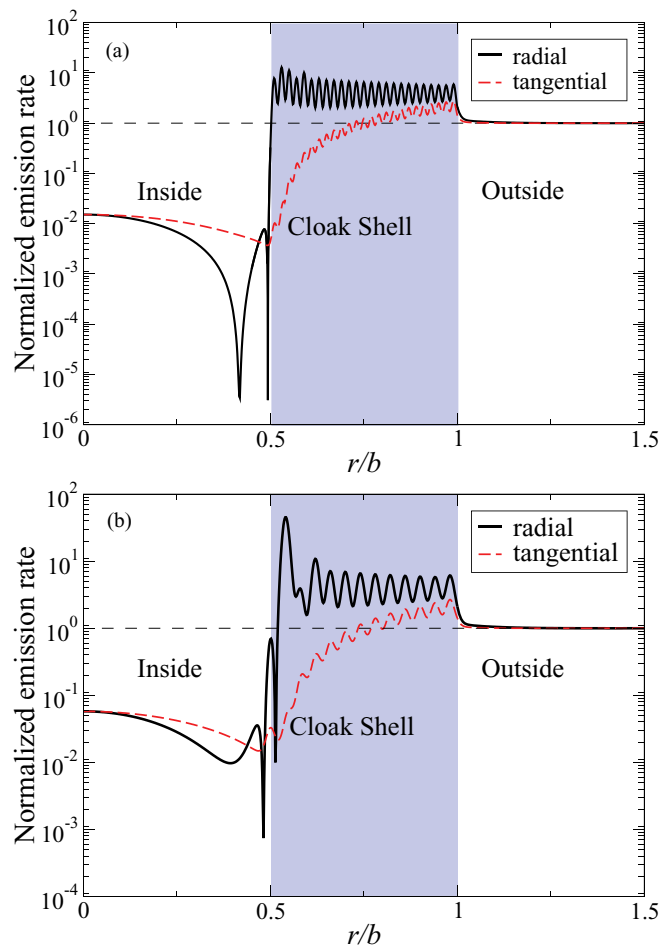
FIG. 3. (Color online) (a) Normalized emission rate as a function of distance from the center of a spherical cloak for an electric dipole, for two orientations, radial (solid line) and tangential (dashed line), of the dipole moment. Parameters: $\lambda = b = 2a$, $d = b/50$. (b) same as (a) for $d = b/25$. The horizontal dashed line marks the free-space emission rate.

When the source is outside of the cloak ($r/b > 1$) the cloak behaves as one would expect, concealing itself from the source. The emission rate of the source in the presence of the cloak is the same as in vacuum, except when the source is very close to the surface of the cloak (about a discretization cell away). This modest rise in the emission rate (by a factor of around 5,) appears because evanescent waves from the source, with a decay constant on the order of d or shorter, begin to "see" the underlying lattice of the cloak. This effect is most pronounced for the radial orientation of the source reflecting the spatial symmetry of the near field of an electric dipole, and the continuity relations for the electric field at an interface.[46,56]

When the source is inside the shell of the cloak ($0.5 < r/b < 1$), we observe rapid oscillations of the emission rate. Note that the magnitude of the emission rate now depends strongly on the orientation of the dipole moment of the source. These oscillations reflect the variation in the local field as the source moves between the discrete elements of the cloak. The amplitude of the local field depends on where the source is with respect to the lattice (see Refs. 48 and 57 for a discussion of local-field effects on emission rates in a simpler lattice

configuration). In the present case, the source is on the x axis and the nearest discrete elements lie in the planes $y = \pm d/2$ and $z = \pm d/2$.

When the source is within the cloaked region ($r/b < 0.5$), the evolution of the emission rate still depends on the orientation of the dipole moment of the source except, of course, at the center of the cloak. Overall, the emission of the source is inhibited by about two orders of magnitude for a tangential orientation. For the radial orientation of the source, we observe a strong inhibition of the emission by about five orders of magnitude for a source inside the cloak, very close to the interface ($r/b \approx 0.5$) and again at a distance $r \approx 0.42b$ from the center. In Fig. 3(b), we show similar calculations to Fig. 3(a) but for a metamaterial whose discrete elements are twice the size, and therefore the total number of elements is roughly eight times smaller. Whereas the magnitude of the emission rate has changed, the overall picture remains qualitatively the same. Emission by the source is inhibited inside the cloak and oscillates within the shell of the cloak due to local-field effects. Because the cloak is formed by significantly fewer discrete elements than in the previous case, it behaves as an even less ideal structure resulting, for instance, in an inhibition at the center of the cloak about four times weaker than in the case of Fig. 3(a).

We see therefore that the emission rate is not uniform inside the cloak, which reveals that the local density of states is not "spatially flat" inside the cloak. The previous calculations only show an overall inhibition of the source by the cloak, which is perhaps expected, however, this is not the full story as the local density of states is also not "spectrally flat." This is evidenced by Fig. 4 where a resonant behavior is observed around a wavelength of $0.8a$ for a source at the center of the cloak. Therefore, at certain frequencies, the cloak can also *enhance* the emission of the source, causing it to radiate more power than it would in free space, which is rather at odds with the spirit of cloaking. In the next section, we provide
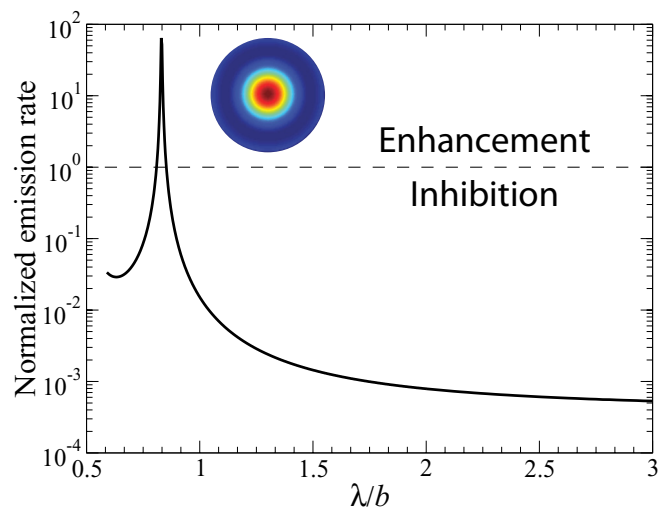

FIG. 4. (Color online) Normalized emission rate as a function of the wavelength for a source at the center of the cloak ($b = 2a$, $d = b/50$). The inset shows the energy density inside the cloak at the peak wavelength $\lambda \approx 0.8b$.

an interpretation of these features in terms of a Purcell effect associated with cavity modes.

IV. PURCELL EFFECT IN A LEAKY CLOAK: ROLE OF RESONANCES

To better understand the origin of the spatial and spectral features of the emission rate we observed in the previous section we turn to a cylindrical cloak. Reducing the spatial dimension allows us to use a finite elements (FE) computation[58] to perform a fine scan in frequency while limiting the computation time. Although the discretization geometry in FE is different to the DDA, the overall principle is the same: a discretized model of the cloak will exhibit leakage between the inside and the outside of the cloak. We treat a cylindrical cloak with geometric parameters still matching the schematic of Fig. 3(a) but with material parameters taken from Eq. (2) in Ref. 5. We consider different locations of the source (electric current line along z) inside the cloak (distance $r < a$ from the center). For each location, we compute the frequency dependence of the emission rate. The result is shown in Fig. 5.

We observe many resonances over the frequency domain considered, showing that the cloak behaves like a (leaky) multimode cavity. Note that Fig. 5 is a spectral plot of the Purcell effect, which depends not only on the spectral overlap between the dipole source and the cavity modes, but on their spatial overlap as well (as illustrated by the dependence of the emission rate, at a given frequency, on the position of the source). For each resonance, we also plot in Fig. 5 the energy density within the cloak (for $r < a$) that clearly shows that the cloak behaves like a cylindrical cavity supporting multiple electromagnetic modes.[37] The enhancement of the emission rate can be now understood in terms of the spectral and spatial couplings of the source with the modes of the cavity. Accordingly, an inhibited emission indicates that the source is unable to couple efficiently to any cavity mode, due to spectral or spatial detuning or both. By extension, we can now interpret the resonance observed for the spherical cloak

in Fig. 3(b) as resulting from the coupling of the source to a mode of the spherical cavity formed by the cloak.

V. PURCELL EFFECT IN A DISPERSIVE AND LOSSY CLOAK

Now that we have discussed the resonance mechanism for a source inside a lossless composite cloak, we introduce material dispersion and losses in the spherical cloak and examine how it affects the radiation dynamics of the source. Assuming a Lorentzian dispersion profile,[59] which is commonly used to model the material dispersion of metamaterial structures,[60] we define

$$\bar{\bar{\epsilon}}_{\text{disp}}(\mathbf{r};\omega) = \left(1 - \frac{\omega_\epsilon \Gamma_\epsilon}{\omega^2 - \omega_\epsilon^2 + i\omega\Gamma_\epsilon}\right)\bar{\bar{\epsilon}}(\mathbf{r}), \quad (5)$$

$$\bar{\bar{\mu}}_{\text{disp}}(\mathbf{r};\omega) = \left(1 - \frac{\omega_\mu \Gamma_\mu}{\omega^2 - \omega_\mu^2 + i\omega\Gamma_\mu}\right)\bar{\bar{\mu}}(\mathbf{r}), \quad (6)$$

where $\bar{\bar{\epsilon}}(\mathbf{r})$ and $\bar{\bar{\mu}}(\mathbf{r})$ are given by Eq. (1) and ω_ϵ (ω_μ) and Γ_ϵ (Γ_μ) are the transition frequency and damping rate for the permittivity (permeability). Equations (5) and (6) satisfy causality and are Kramers-Kronig consistent.[59,61] By inserting these new permittivity and permeability tensors in the expressions of the electric and magnetic polarizabilities [see Eqs. (2) and (3)], we have a model of a composite, dispersive, lossy cloak.

With material losses, there is now a nonradiative decay channel for the source. For our purpose, we define as nonradiative decay that part of the power lost by the source that does not emerge as radiation in the far field. Note, however, that our definition of nonradiative losses comprises both the contribution from the nonradiative energy transfer associated with the longitudinal field of the source[62] and the contribution from the partial absorption of the transverse field as it travels through the absorbing medium forming the cloak.

We plot in Fig. 6 the total [see Eq. (4)], radiative (far-field power), and nonradiative (difference between the previous two quantities) decay rates (normalized to the decay rate in
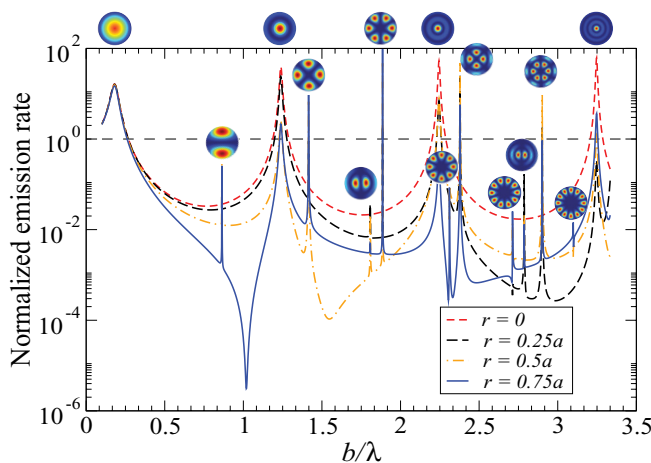

FIG. 5. (Color online) Normalized decay rate as a function of frequency for a source located at a distance r from the center of a cylindrical cloak. For each resonance, the corresponding map of the energy density is shown.
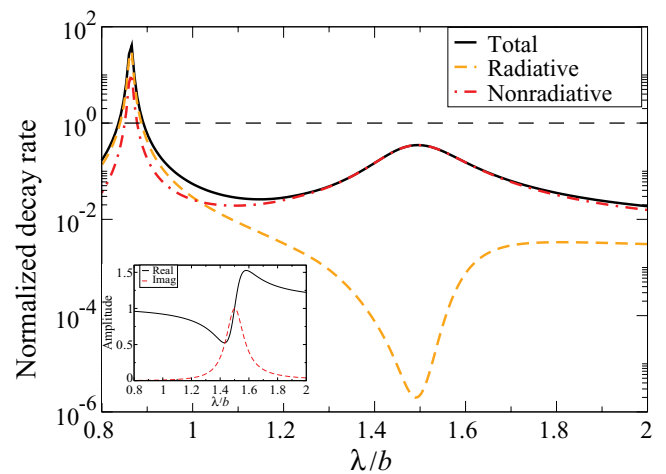

FIG. 6. (Color online) Total, radiative, and nonradiative decay rates for an electric dipole source at the center of a dispersive, lossy, composite cloak with $d = a/25$ and $\omega_\epsilon = \omega_\mu = \omega_g = 2\pi c/(1.5a)$; $\Gamma_\epsilon = \Gamma_\mu = \omega_g/10$. The inset shows the real and imaginary parts of the dispersion profile.
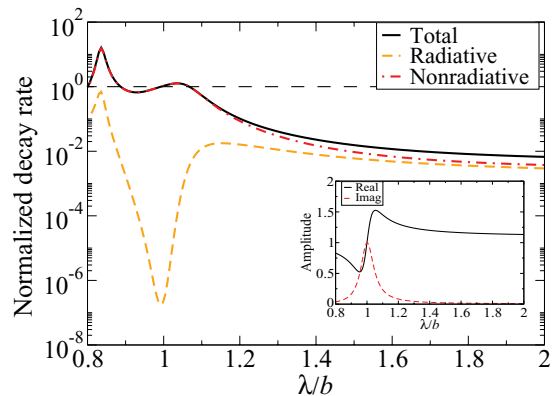
FIG. 7. (Color online) Same as Fig. 6 with $\omega_\epsilon = \omega_\mu = \omega_g = 2\pi c/a$.

vacuum) for a source at the center of a composite spherical cloak with $d = a/25$ and with dispersion parameters as given in the caption. The peak of absorption for both the permittivity and permeability occur at $\lambda = 1.5a$. At this wavelength, we now observe an increase in the total decay rate, however, this increase originates exclusively from nonradiative energy transfer from the source to the cloak. In fact, as shown in Fig. 6, the radiative decay rate, which corresponds to the power radiated to the far field (outside of the cloak) by the source, goes down by several orders of magnitude around the wavelength corresponding to the absorption peak. To an external observer, radiation by the source would appear to be strongly suppressed near the absorption peak, however, this does not necessarily mean that the cloaking mechanism is efficient as the predominantly nonradiative decay rate reveals that most of the energy lost by the source would end up as heat in the cloak. An observer could then, in principle, detect the thermal signature of the combined cloak and source system.

As we move away from the absorption peak, we observe two qualitatively different behaviors. For larger wavelengths, the nonradiative decay mechanism still dominates even as the material losses decrease. This is because in the long-wavelength regime the decay process is dominated by the longitudinal field, thus promoting nonradiative energy transfer.[62] On the shorter wavelength side of the absorption peak, we observe a marked increase in the radiative decay rate, which overcomes the nonradiative rate near the cavity resonance peak. This is because the coupling of the source to the cavity mode via the transverse field promotes radiation by the source. As we are far enough from the absorption peak, material losses are not able to overcome the cavity enhanced radiative decay.

The picture changes when the absorption peak is closer to the cavity resonance as shown in Fig. 7, where the peak of absorption for both the permittivity and permeability occur at $\lambda = a$. In this case, nonradiative processes dominate over the entire spectral range under consideration. Even at the cavity

resonance, the decay is predominantly nonradiative as the cavity resonance is unable to overcome the material losses. Note that at the peak of absorption, our level of loss is actually higher than values that have been achieved experimentally with state of the art metamaterial structures,[63] therefore our calculations can be considered conservative.

VI. CONCLUSION

In conclusion, we have investigated radiation dynamics in a composite invisibility cloak. The main consequence of having a discrete, and therefore nonideal cloak is to introduce an electromagnetic coupling, or leakage, between the inside of the cloak and the outside world. As a result, while a source outside the cloak ($r > b$) would radiate at the same rate as in free space, a source inside the cloak ($r < a$) can have its emission inhibited or *enhanced* by several orders of magnitude depending on how well the source couples to the leaky modes inside the cloak. In particular, when the spectral and spatial overlap between the source and a cavity resonance are optimal, the source can radiate more than it would in free space in the absence of the cloak. Hence the "invisibility" cloak acts more like a supervisibility device. Another consequence of the discrete nature of the cloak is that a source placed inside the shell of the cloak ($a < r < b$) can also have its emission rate altered by local-field effects. Of course, in an experiment, the exact spatial dependence and strength of these local-field effects would depend on the specific nature and (discrete) geometry of the underlying metamaterial structure.

One consequence of these results is that the very limitations of current metamaterial technology, which requires discrete structures and hinders perfect cloaking, can be exploited to design novel discrete cavities to control the radiative energy losses of a source at frequencies where standard cavity designs may not be suitable. Of course, absorption is likely to be present in an actual device, thereby opening a nonradiative decay channel for the source. However, how strong an effect material losses will have on the radiation dynamics of the source will be determined mainly by the competition between the cavity-induced enhancement of radiative decay (Purcell effect) and the nonradiative energy transfer mediated by the longitudinal field of the source. Assuming that absorption levels are fixed, because the dominant channel for nonradiative decay is via the longitudinal field of the source, nonradiative decay can be mitigated by placing the source more than a wavelength away from the lossy cavity walls and optimizing its spectral and spatial overlap with a cavity mode. Note that all our conclusions hold for a magnetic dipole source as well. Finally, let us note that although we have focused our attention on the dissipative part of the source-field coupling (emission rate), the dispersive part of the coupling (i.e., the frequency shift)[46] will also be altered by the leaky modes of the composite cloak.

---

[1]E. M. Purcell, Phys. Rev. **69**, 681 (1946).

[2]S. Haroche, in *Fundamental Systems in Quantum Optics*, edited by J. Dalibard, J. M. Raimond, and J. Zinn-Justin (North-Holland, Amsterdam, 1992), pp. 767–940.

[3]U. Leonhardt, Science **312**, 1777 (2006).

[4]J. B. Pendry, D. Schurig, and D. R. Smith, Science **312**, 1780 (2006).

[5]D. Schurig, J. J. Mock, B. J. Justice, S. A. Cummer, J. B. Pendry, A. F. Starr, and D. R. Smith, Science **314**, 977 (2006).

[6] I. I. Smolyaninov, V. N. Smolyaninova, A. V. Kildishev, and V. M. Shalaev, Phys. Rev. Lett. **102**, 213901 (2009).

[7] B. Zhang, Y. Luo, X. Liu, and G. Barbastathis, Phys. Rev. Lett. **106**, 033901 (2011).

[8] X. Chen, Y. Luo, J. Zhang, K. Jiang, J. B. Pendry, and S. Zhang, Nat. Commun. **2**, 176 (2011).

[9] H. Chen and B. Zheng, Sci. Rep. **2**, 255 (2012).

[10] G. W. Milton, N.-A. P. Nicorovici, R. C. McPhedran, and V. A. Podolskiy, Proc. R. Soc. London, Ser. A **461**, 3999 (2005).

[11] G. W. Milton and N.-A. P. Nicorovici, Proc. R. Soc. London, Ser. A **462**, 3027 (2006).

[12] N. A. Nicorovici, G. W. Milton, R. C. McPhedran, and L. C. Botten, Opt. Express **15**, 6314 (2007).

[13] O. P. Bruno and S. Lintner, J. Appl. Phys. **102**, 124502 (2007).

[14] A. Alù and N. Engheta, Phys. Rev. E **72**, 016623 (2005).

[15] B. Edwards, A. Alù, M. G. Silveirinha, and N. Engheta, Phys. Rev. Lett. **103**, 153901 (2009).

[16] D. Rainwater, A. Kerkhoff, K. Melin, J. C. Soric, G. Moreno, and A. Alù, New J. Phys. **14**, 013054 (2012).

[17] A. Greenleaf, Y. Kurylev, M. Lassas, and G. Uhlmann, Commun. Math. Phys. **275**, 749 (2007).

[18] W. Cai, U. Chettiar, A. Kildishev, V. Shalaev, and G. Milton, Appl. Phys. Lett. **91**, 111105 (2007).

[19] W. Cai, U. K. Chettiar, A. V. Kildishev, and V. M. Shalaev, Opt. Express **16**, 5444 (2008).

[20] J. Li and J. B. Pendry, Phys. Rev. Lett. **101**, 203901 (2008).

[21] R. Liu, C. Ji, J. J. Mock, J. Y. Chin, T. J. Cui, and D. R. Smith, Science **323**, 366 (2009).

[22] H. F. Ma and T. J. Cui, Nat. Commun. **1**, 21 (2010).

[23] J. Valentine, J. Li, T. Zentgraf, G. Bartal, and X. Zhang, Nat. Mater. **8**, 568 (2009).

[24] L. H. Gabrielli, J. Cardenas, C. B. Poitras, and M. Lipson, Nat. Photon. **3**, 461 (2009).

[25] J. H. Lee, J. Blair, V. A. Tamma, Q. Wu, S. J. Rhee, C. J. Summers, and W. Park, Opt. Express **17**, 12922 (2009).

[26] T. Ergin, N. Stenger, P. Brenner, J. B. Pendry, and M. Wegener, Science **328**, 337 (2010).

[27] N. Landy and D. R. Smith, Nat. Mater. **12**, 25 (2013).

[28] J. Fischer, T. Ergin, and M. Wegener, Opt. Lett. **36**, 2059 (2011).

[29] A. Alù and N. Engheta, Phys. Rev. Lett. **102**, 233901 (2009).

[30] C. Argyropoulos, P.-Y. Chen, F. Monticone, G. D'Aguanno, and A. Alù, Phys. Rev. Lett. **108**, 263905 (2012).

[31] Z. Ruan, M. Yan, C. W. Neff, and M. Qiu, Phys. Rev. Lett. **99**, 113903 (2007).

[32] M. Yan, Z. Ruan, and M. Qiu, Phys. Rev. Lett. **99**, 233901 (2007).

[33] M. Yan, Z. Ruan, and M. Qiu, Opt. Express **15**, 17772 (2007).

[34] A. Greenleaf, Y. Kurylev, M. Lassas, and G. Uhlmann, Phys. Rev. Lett. **101**, 220404 (2008).

[35] A. Greenleaf, Y. Kurylev, M. Lassas, and G. Uhlmann, Phys. Rev. E **83**, 016603 (2011).

[36] S. Guenneau, R. C. McPhedran, S. Enoch, A. B. Movchan, M. Farhat, and N.-A. P. Nicorovici, J. Opt. **13**, 024014 (2011).

[37] M. Farhat, P.-Y. Chen, S. Guenneau, S. Enoch, R. McPhedran, C. Rockstuhl, and F. Lederer, Phys. Rev. B **84**, 235105 (2011).

[38] B. Zhang, H. Chen, B.-I. Wu, and J. A. Kong, Phys. Rev. Lett. **100**, 063904 (2008).

[39] W. Cai and V. Shalaev, *Optical Metamaterials: Fundamentals and Applications* (Springer, New York, London, 2009).

[40] U. Leonhardt, *Essential Quantum Optics: From Quantum Measurements to Black Holes* (Cambridge University Press, Cambridge, 2010).

[41] E. M. Purcell and C. R. Pennypacker, Astrophys. J. **186**, 705 (1973).

[42] B. T. Draine, Astrophys. J. **333**, 848 (1988).

[43] P. C. Chaumet, A. Rahmani, F. Zolla, A. Nicolet, and K. Belkebir, Phys. Rev. A **84**, 033808 (2011).

[44] P. C. Chaumet, A. Rahmani, F. Zolla, and A. Nicolet, Phys. Rev. E **85**, 056602 (2012).

[45] A. Rahmani, P. C. Chaumet, and F. de Fornel, Phys. Rev. A **63**, 023819 (2001).

[46] A. Rahmani and G. W. Bryant, Phys. Rev. A **65**, 033817 (2002).

[47] F. Bordas, N. Louvion, S. Callard, P. C. Chaumet, and A. Rahmani, Phys. Rev. E **73**, 056601 (2006).

[48] A. Rahmani, P. C. Chaumet, and G. W. Bryant, Opt. Express **18**, 8499 (2010).

[49] D. Schurig, J. Pendry, and D. Smith, Opt. Express **14**, 9794 (2006).

[50] P. C. Chaumet and A. Rahmani, Opt. Lett. **34**, 917 (2009).

[51] Y. You, G. W. Kattawar, P.-W. Zhai, and P. Yang, Opt. Express **16**, 2068 (2008).

[52] G. S. Agarwal, Phys. Rev. A **11**, 230 (1975).

[53] J. M. Wylie and J. E. Sipe, Phys. Rev. A **30**, 1185 (1984).

[54] R. C. McPhedran, L. C. Botten, J. McOrist, A. A. Asatryan, C. M. de Sterke, and N. A. Nicorovici, Phys. Rev. E **69**, 016609 (2004).

[55] V. Ginis, P. Tassin, C. M. Soukoulis, and I. Veretennicoff, Phys. Rev. B **82**, 113102 (2010).

[56] P. C. Chaumet, A. Rahmani, F. de Fornel, and J.-P. Dufour, Phys. Rev. B **58**, 2310 (1998).

[57] A. Rahmani, P. C. Chaumet, and G. W. Bryant, Opt. Lett. **27**, 430 (2002).

[58] COMSOL Multiphysics - http://www.comsol.com/.

[59] J. D. Jackson, *Classical Electrodynamics*, 2nd ed. (Wiley, New York, 1975).

[60] H. Chen, Z. Liang, P. Yao, X. Jiang, H. Ma, and C. T. Chan, Phys. Rev. B **76**, 241104 (2007).

[61] J. Leng, J. Opsal, H. Chu, M. Senko, and D. Aspnes, Thin Solid Films **313**, 132 (1998).

[62] S. M. Barnett, B. Huttner, R. Loudon, and R. Matloob, J. Phys. B **29**, 3763 (1996).

[63] C. M. Soukoulis and M. Wegener, Nat. Photon. **5**, 523 (2011).